ELSEVIER

Journal of Photochemistry and Photobiology A: Chemistry 145 (2001) 135–141

Journal of Photochemistry and Photobiology A:Chemistry

www.elsevier.com/locate/jphotochem

Sensitization of nanocrystalline TiO_2 film by ruthenium(II) diimine dithiolate complexes

Ashraful Islam, Hideki Sugihara*, Kohjiro Hara, Lok Pratap Singh, Ryuzi Katoh, Masatoshi Yanagida, Yoshiaki Takahashi, Shigeo Murata, Hironori Arakawa[1]

National Institute of Advanced Industrial Science and Technology (AIST), Photoreaction Control Research Center, AIST Tsukuba Central 5, 1-1 Higashi, 1-Chome, Tsukuba, Ibaraki 305-8565, Japan

Received 14 May 2001; received in revised form 21 June 2001; accepted 4 July 2001

Abstract

A new series of ruthenium(II) polypyridyl sensitizers with strongly electron donating dithiolate ligands $Ru(dcbpy)_2(L)$ and $Ru(dcphen)_2(L)$ where L is quinoxaline-2,3-dithiolate (qdt) or ethyl-2-cyano-3,3-dimercaptoacrylate (ecda) or 1,2-benzenedithiolate (bdt) or 3,4-toluenedithiolate (tdt), dcbpy is 4,4′-dicarboxy-2,2′-bipyridine, and dcphen is 4,7-dicarboxy-1,10-phenanthroline have been prepared for sensitization of nanocrystalline TiO_2 electrodes. All the complexes exhibit a broad metal-to-ligand charge transfer absorption band over the whole visible range. The low-energy absorption bands and the Ru(II)/(III) oxidation potentials in these complexes could be tuned to about 150 nm and 600 mV, respectively, by choosing appropriate dithiolate ligands. When anchored to nanocrystalline titanium dioxide electrodes for light to electrical energy conversion in regenerative photoelectrochemical cells with I^-/I_3^- acetonitrile electrolyte, these complexes show different sensitization to TiO_2 electrodes with increasing activity in the sequence L = tdt, bdt, ecda, qdt. Both $Ru(dcbpy)_2(qdt)$ and $Ru(dcphen)_2(qdt)$ show overall cell efficiency (η) of about 3–4%, due to incident photon to current conversion efficiency of around 40–45% at 500 nm. The low cell efficiency of ecda complexes may be due to slow regeneration of the dye by electron donation from iodide following charge injection into TiO_2.

Keywords: Photosensitizer; Ruthenium complexes; Dithiolate; Solar cell

1. Introduction

Photoelectrochemical systems with dye-sensitized metal oxide semiconductor electrodes have allowed the construction of low-cost photovoltaic devices over past two decades [1]. In the 1990s, a major photoelectrochemical solar cell development was obtained with the introduction of fractal thin film dye sensitized solar cells devised by O'Regan and Grätzel [2]. In this solar cell, a monolayer of dye is attached to the surface of nanocrystalline film. Photoexcitation of the dye results in the injection of an electron into the conduction band of the oxide. The original state of the dye is subsequently restored by electron donation from a redox system, such as the iodide/tri-iodide couple. In order to be useful in such a cell, the sensitizer should fulfill several requirements, including: (i) the dye's absorption spectrum should overlap with the solar spectrum in order to get maximum power conversion, (ii) the excited state should have enough thermodynamic driving force for the injection of electrons into the conduction band, (iii) the redox potential should be sufficiently positive so that the neutral sensitizer can be regenerated via electron donation from the redox electrolyte and (iv) the oxidized sensitizer should be stable, in order to be quantitatively reduced back by an electron.

Several organic dyes [1,3–5] and transition metal complexes of Ru(II) [2,6–9], Os(II) [10,11], Pt(II) [12], Fe(II) [13], Re(I) [14] and Cu(I) [15] have been employed in the solar cells to sensitize nanocrystalline metal oxide semiconductors. So far, the most successful sensitizers employed in these devices are polypyridyl complexes of ruthenium(II) anchored to nanocrystalline TiO_2 films [2,6,9,16]. The metal-to-ligand charge transfer (MLCT) absorption of ruthenium(II) polypyridyl complexes can be extended to longer wavelengths by introducing a diimine ligand with a lower-lying π^* molecular orbital (LUMO) or by destabilization of the Ru t_{2g} (HOMO) orbital with a strongly donating ligand. Recently, we have tuned the MLCT transitions up to 600 nm in Ru-diimine sensitizers by introducing a ligand with a low π^* orbital, such as 4,4′-dicarboxy-2,2′-biquinoline (dcbiq) [17]. But the sensitizers did not perform efficiently due

* Corresponding author. Tel.: +81-298-61-4641; fax: +81-298-61-4496.
E-mail address: sugihara-hideki@aist.go.jp (H. Sugihara).
[1] Co-corresponding author.

1010-6030/01/$ – see front matter
PII: S1010-6030(01)00575-5

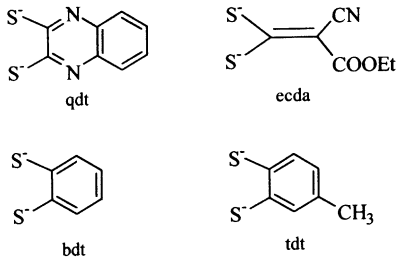

Scheme 1.

to a poor charge injection to the conduction band of the TiO_2. Ruthenium(II) polypyridyl complexes of the type $RuL_2(NCS)_2$ and $RuL'(NCS)_3$ where L = 4,4′-dicarboxy-2,2′-bipyridine (dcdpy) [2,6] or 4,7-dicarboxy-1,10-phenanthroline (dcphen) [18] and L′ = 4,4′,4″-tricarboxy-2,2′:6′,2″-terpyridine (tcterpy) [19] exhibit exceptionally high solar light-to-electrical energy conversion efficiency. The role of the monodentate thiocyanato ligands is to tune the spectral and redox properties of the sensitizers by destabilization of the metal t_{2g} orbital. The presence of monodentate donor ligands (NCS^-) can undergo ligand photosubstitution or photodegradation reaction via population of an upper lying ligand field excited state and these processes can be reduced by multidentate ligands. Bignozzi and coworkers [7,20] have utilized different dithiocarbamates and triazole-type donor ligands as nonchromophoric chelating ligands to tune sensitizer absorption properties and efficiently sensitize TiO_2 beyond 700 nm. Recently, Takahashi et al. [21] have reported an efficient ruthenium(II) polypyridyl sensitizer containing one bidentate β-diketonato ligand. In our previous studies, we have demonstrated that square planar platinum(II) diimine complexes containing donor dithiolate ligands can sensitize nanocrystalline TiO_2 [12]. We report here the synthesis, photophysical, and photoelectrochemical properties of complexes of the type $Ru(dcbpy)_2(L)$ and $Ru(dcphen)_2(L)$ where L is one of the four dithiolate ligands shown in Scheme 1: quinoxaline-2,3-dithiolate (qdt), ethyl-2-cyano-3,3-dimercaptoacrylate (ecda), 1,2-benzenedithiolate (bdt), and 3,4-toluenedithiolate (tdt). Here, we have tuned the MLCT transitions up to 700 nm using the above four dithiolate ligands.

2. Experimental details

2.1. Materials

1,2-Benzenedithiol (H_2bdt), 3,4-toluenedithiol (H_2tdt) and $RuCl_3 \cdot xH_2O$ were used as received. 4,4′-Dicarboxy-2,2′-bipyridine (dcbpy), 4,7-dicarboxy-1,10-phenanthroline (dcphen) [18], ethyl-2-cyano-3,3-dimercaptoacrylate dipotassium salt (K_2ecda) [22], quinoxaline-2,3-dithiol (H_2qdt) [23], $Ru(dcbpy)_2Cl_2$ [6] and $Ru(dcphen)_2Cl_2$ [18] were prepared according to literature methods.

2.1.1. Synthesis of metal complexes

The complexes containing the dithiolate ligands were prepared by the following procedure. The $Ru(dcbpy)_2Cl_2$ or $Ru(dcphen)_2Cl_2$ (3.0×10^{-4} M) complex was placed in a round-bottom flask containing 40 ml of degassed methanol and dissolved by a minimum amount of 0.1 M KOH. To this was added a degassed solution of dithiolate (3.5×10^{-4} M) in 10 ml of MeOH. The reaction mixture was then heated to reflux with vigorous stirring for 5 h under Ar atmosphere. Then the reaction mixture was allowed to cool, and the solvent was removed on a rotary evaporator. The resulting solid was dissolved in water, the solution was filtered and the product was precipitated by addition of 0.1 M HNO_3. The product was redissolved in minimum amount of aqueous 0.1 M tetrabutylammonium hydroxide (TBAOH) and purified by column chromatography using Sephadex LH-20 as a column support and water as eluent. Isolation of the product after chromatography was achieved by adjusting the pH with 0.1 M HNO_3. The resulting precipitate was collected by filtration, washed several times with water and dried under vacuum.

*Ru(dcbpy)$_2$(qdt) (**1**).* Yield 55%. MS (ESIMS): *m/z*: 259.3 $(M-3H)^{3-}$, 389.6 $(M-2H)^{2-}$. ^{1}H NMR (300 MHz, D_2O–NaOD): δ 9.42 (H, d, J = 5.1 Hz), 8.66 (H, s), 8.59 (2H, m), 8.52 (H, s), 8.06 (H, d, J = 6.9 Hz), 7.73 (2H, d, J = 6.0 Hz), 7.62 (H, d, J = 5.7 Hz), 7.53 (H, d, J = 5.7 Hz), 7.40 (H, d, J = 5.6 Hz), 7.29 (H, d, J = 7.2 Hz), 7.24 (H, d, J = 5.4 Hz), 7.07 (H, t, J = 6.0 Hz), 6.69 (H, t, J = 6.1 Hz), 5.70 (H, d, J = 8.4 Hz). Anal. Calcd. for $C_{32}H_{20}N_6O_8S_2Ru \cdot (H_2O)_4$: C, 45.02; H, 3.31; N, 9.84; S, 7.51. Found: C, 45.28; H, 3.40; N, 9.71; S, 7.45.

*Ru(dcphen)$_2$(qdt) (**2**).* Yield 50%. MS (ESIMS): *m/z*: 275.8 $(M-3H)^{3-}$, 413.5 $(M-2H)^{2-}$, 424.8 $(M-3H+Na)^{2-}$. ^{1}H NMR (300 MHz, D_2O–NaOD): δ 9.75 (H, d, J = 5.7 Hz), 8.42 (H, d, J = 5.7 Hz), 8.31–8.17 (4H, m), 7.87 (H, d, J = 5.1 Hz), 7.80 (H, d, J = 5.4 Hz), 7.72 (H, d, J = 5.7 Hz), 7.60 (H, d, J = 5.4 Hz), 7.27 (2H, t, J = 7.8 Hz), 7.13 (H, d, J = 5.7 Hz), 7.00 (H, t, J = 7.2 Hz), 6.52 (H, t, J = 6.6 Hz), 5.57 (H, d, J = 7.8 Hz). Anal. Calcd. for $C_{36}H_{20}N_6O_8S_2Ru \cdot (H_2O)_5$: C, 47.01; H, 3.29; N, 9.14; S, 6.97. Found: C, 47.30; H, 3.35; N, 9.03; S, 6.88.

*Ru(dcbpy)$_2$(ecda) (**3**).* Yield 60%. MS (ESIMS): *m/z*: 257.7 $(M-3H)^{3-}$, 387.4 $(M-4H+Na)^{3-}$, 387.4 $(M-2H)^{2-}$, 398.3 $(M-3H+Na)^{2-}$. ^{1}H NMR (300 MHz, D_2O–NaOD): δ 9.53 (2H, d, J = 5.1 Hz), 8.62 (2H, s), 8.48 (2H, s), 7.83 (2H, d, J = 5.4 Hz), 7.63 (2H, d, J = 3.6 Hz), 7.22 (2H, d, J = 5.1 Hz), 3.91 (2H, d, J = 7.5 Hz), 0.93 (3H, m). Anal. Calcd. for $C_{30}H_{21}N_5O_{10}S_2Ru \cdot (H_2O)_4$: C, 42.45; H, 3.44; N, 8.25; S, 7.56. Found: C, 43.30; H, 3.38; N, 8.12; S, 7.42.

*Ru(dcphen)$_2$(ecda) (**4**).* Yield 55%. MS (ESIMS): *m/z*: 273.92 $(M-3H)^{3-}$, 411.38 $(M-2H)^{2-}$. ^{1}H NMR (300 MHz, D_2O–NaOD): δ 9.81 (2H, d, J = 5.4 Hz), 8.29 (2H, d, J = 9.6 Hz), 8.16 (2H, d, J = 9.6 Hz), 7.89 (2H, d, J = 5.1 Hz), 7.80 (2H, d, J = 5.1 Hz), 7.14 (2H, d, J = 5.4 Hz), 3.92 (2H, d, J = 5.4 Hz), 0.93 (3H, t, J = 5.4 Hz). Anal. Calcd. for $C_{34}H_{21}N_5O_{10}S_2Ru \cdot (H_2O)_4$: C, 45.53; H, 3.26; N, 7.81; S, 7.15. Found: C, 45.65; H, 3.38; N, 7.62; S, 7.22.

Ru(dcbpy)$_2$(bdt) (**5**). Yield 50%. MS (ESIMS): *m/z*: 252.5 $(M-3H + MeOH)^{3-}$, 379.8 $(M-2H + MeOH)^{2-}$, 760.9 $(M - H + MeOH)^{-}$. ^{1}H NMR (500 MHz, D_2O–NaOD): δ 9.65 (H, d, $J = 7.5$ Hz), 9.15 (H, d, $J = 7.5$ Hz), 8.58 (2H, s), 8.54 (2H, s), 7.73 (H, d, $J = 7.0$ Hz), 7.63 (2H, t, $J = 7.5$ Hz), 7.45 (H, d, $J = 6.5$ Hz), 7.39 (H, d, $J = 7.0$ Hz), 7.36 (H, d, $J = 7.0$ Hz), 7.32 (H, d, $J = 9.5$ Hz), 7.27 (H, d, $J = 7.0$ Hz), 7.02 (H, t, $J = 7.0$ Hz), 6.93 (H, t, $J = 7.5$ Hz).

Ru(dcbpy)$_2$(tdt) (**6**). Yield 55%. MS (ESIMS): *m/z*: 257.5 $(M-3H+MeOH)^{3-}$, 386.9 $(M-2H+MeOH)^{2-}$. ^{1}H NMR (300 MHz, D_2O–NaOD): δ 9.66 (H, d, $J = 5.7$ Hz), 9.15 (H, d, $J = 5.4$ Hz), 8.58 (2H, s), 8.54 (2H, s), 7.72 (H, d, $J = 5.7$ Hz), 7.63 (2H, t, $J = 5.7$ Hz), 7.45 (H, d, $J = 5.7$ Hz), 7.36 (2H, t, $J = 8.4$ Hz), 7.21 (H, d, $J = 7.8$ Hz), 7.09 (H, s), 6.77 (H, d, $J = 7.8$ Hz), 2.07 (3H, m). Anal. Calcd. for $C_{31}H_{22}N_4O_8S_2Ru\cdot(H_2O)_4$: C, 45.64; H, 3.71; N, 6.87; S, 7.86. Found: C, 46.02; H, 3.80; N, 6.89; S, 7.71.

Ru(dcphen)$_2$(tdt) (**7**). Yield 55%. MS (ESIMS): *m/z*: 272.8 $(M-3H + MeOH)^{3-}$, 410.7 $(M-2H + MeOH)^{2-}$ ^{1}H NMR (300 MHz, D_2O–NaOD): δ 10.00 (H, d, $J = 5.7$ Hz), 9.29 (H, d, $J = 5.7$ Hz), 8.12–8.23 (4H, m), 7.91 (H, d, $J = 5.1$ Hz), 7.69 (3H, t, $J = 5.4$ Hz), 7.52 (H, d, $J = 5.1$ Hz), 7.30 (2H, m), 7.21 (2H, d, $J = 6.6$ Hz), 2.07 (3H, m). Anal. Calcd. for $C_{35}H_{22}N_4O_8S_2Ru\cdot(H_2O)_3$: C, 49.70; H, 3.34; N, 6.62; S, 7.58. Found: C, 49.02; H, 3.31; N, 6.54; S, 7.75.

2.2. Methods

UV–Vis and emission spectra were recorded on a Shimadzu UV-3101PC spectrophotometer and a Hitachi F-4500 spectrophotometer, respectively. The measured emission spectra were corrected for detector sensitivity using a standard tungsten lamp as the reference source. The emission lifetimes were measured by exciting the sample with a ~7 ns pulse at 500 nm from an optical parametric oscillator (Surelite OPO) pumped at 355 nm by a Nd:YAG laser (Continum Surelite II). The emission decay was followed on a Tektronix TDS680C digitizing signal analyzer, having used a Hamamatsu R928 photomultiplier to convert the light signal to a voltage signal. ^{1}H NMR spectra were recorded by a Varian 300BB spectrometer. Electrospray ionization mass spectra (ESIMS) were obtained on a Micromass Quattro II mass spectrometer. Cyclic voltammograms were collected using a BAS-100 electrochemical analyzer (Bioanalytical System). The counter electrode was a platinum wire, the working electrode was a carbon or platinum disk and the reference electrode was a Ag/AgCl (saturated aqueous KCl) in contact with a KCl salt bridge. Methanol was used as a solvent and the supporting electrolyte was 0.1 M tetrabutylammonium perchlorate.

Thin-layer films. Nanoporous TiO_2 semiconductor thin films of about 16 μm thick on F-doped SnO_2 electrodes were prepared using a previously published procedure [24]. The thin films were coated for 24 h in 5×10^{-5} M ethanolic dye solutions at room temperature. The amount of adsorbed dye was determined by desorbing the dye from an oxide semiconductor film into a solution of 10^{-4} M NaOH in EtOH and measuring the absorption spectrum of the solution.

Photoelectrochemical measurements. Photoelectrochemical measurements were performed in a two-electrode sandwich cell configuration as previously reported [8]. As electrolyte, a mixture containing 0.6 M 1,2-dimethyl-3-propylimidazolium iodide (DMPII), 50 mM I_2, 0.5 M 4-*tert*-butylpyridine (TBP), 0.1 M LiI in acetonitrile was used. The working electrode was illuminated through a conducting glass and the illuminated surface area was 0.25 cm^2.

The photocurrent and photovoltage were measured under simulated solar light (Wacom, WXS-80C-3, AM 1.5, 100 mW/cm^2) using a potentiostat with a nonresistance ammeter (Nikko Keisoku, NPGS-2501). Monochromatic illumination was obtained using a 500 W halogen lamp (Ushio Denki) in combination with a grating monochromator model (Jasco, CT-10), a scanning controller (Jasco, SMD-25C), and a multimeter (Keithley, 2000). The light intensities of monochromatic and solar simulated light were estimated with an optical power meter (Advantest, TQ8210) and a thermopile (The Eppley Lab., Newort, RI), respectively.

3. Results and discussion

3.1. Photophysical properties

The absorption, emission and electrochemical properties of complexes **1**–**7** are summarized in Table 1. The absorption spectra of complexes **1**, **3** and **6** in ethanol–methanol solution are shown in Fig. 1 together with that of Ru(dcbpy)$_2$(NCS)$_2$ (**8**) complex for comparison. All the ruthenium(II) complexes presented show intense UV bands at 281–313 nm and they are assigned to the intraligand π–π* transition of 4,4′-dicarboxy-2,2′-bipyridine or 4,7-dicarboxy-1,10-phenanthroline ligand. Intense and broad MLCT bands are observed in the visible region (Fig. 1). The position of the lower energy MLCT band maximum varies between 517 (**1**) and 670 nm (**7**) where the molar absorption coefficient is in the range from 2000 to 13,000 M^{-1} cm^{-1} (Table 1). As discussed earlier, the key requirement for an efficient sensitizer is that the dye absorption should overlap with the solar emission spectrum in order to get maximum power conversion. This can be achieved either by introducing an acceptor diimine ligand with a LUMO or by destabilization of the metal t_{2g} orbital with increasing donor properties of the dithiolate ligand. In this study, we have tuned the low-energy MLCT absorption band of the complexes **1**–**7** by ca. 150 nm with variation of the dithiolate ligands having different electron-donating strengths (Table 1). The energy of the MLCT transition in these complexes decreases in the following order qdt > ecda > bdt > tdt. The low energy MLCT absorption bands of ecda complexes are red-shifted from that of Ru(dcbpy)$_2$(NCS)$_2$ complex, which is one of the most efficient sensitizers known so far [6]. The bdt

Table 1
Absorption, luminescence and electrochemical properties of the Ru(diimine)$_2$(dithiolate) sensitizers

Sensitizer	Absorption[a]	λ_{max} (nm)	$\varepsilon \times 10^{-3}$ ($M^{-1}cm^{-1}$)	Emission[a]		$E(Ru^{3+/2+})$[b] vs. SCE	$E^*(Ru^{3+/2+})$[c] vs. SCE
				λ_{max} (nm)	τ (ns)		
1 Ru(dcbpy)$_2$(qdt)	310 (25.8)	403 (9.4)	476 (8.6), 517 (8.8)	870	12	+0.84	−0.93
2 Ru(dcphen)$_2$(qdt)	281 (30.1)	405 (6.4)	477 (9.5), 517[d] (9.2)	890	10	+0.86	−0.96
3 Ru(dcbpy)$_2$(ecda)	313 (32.1)	402 (17.5)	500[d] (8.4), 582 (9.8)	925	23	+0.46	−1.14
4 Ru(dcphen)$_2$(ecda)	289 (42.1)	400 (10.0)	477 (12.4), 574 (13.4)	920	50	+0.47	−1.23
5 Ru(dcbpy)$_2$(bdt)	309 (32.3)	463 (9.5)	662 (2.1)	>950	<7	+0.30	−1.16[e]
6 Ru(dcbpy)$_2$(tdt)	307 (32.0)	470 (9.6)	670 (2.0)	>950	<7	+0.28	−1.18[e]
7 Ru(dcphen)$_2$(tdt)	284 (40.2)	425 (12.2)	670 (2.7)	>950	<7	+0.27	−1.19[e]
8 Ru(dcbpy)$_2$(NCS)$_2$[f]	313 (31.2)	396 (14.0)	534 (14.2)	755	50	+0.85	−1.0

[a] In ethanol–methanol (4:1) solution at room temperature.
[b] Half-wave potentials assigned to the $Ru^{3+/2+}$ couple for the sensitizers.
[c] Calculated from $E^*(Ru^{3+/2+}) = E(Ru^{3+/2+}) - E^{0-0}$; E^{0-0} values were estimated from the crossing point of the emission and absorption spectra, when the most intense MLCT absorption band and the emission peak were adjusted to the same height.
[d] Appeared as a shoulder.
[e] E^{0-0} values were estimated from the low energy region tail of the absorption spectra.
[f] Data taken from Refs. [6,18].

and tdt complexes exhibit a broad MLCT absorption band centered at around 670 nm and can absorb entire visible solar emission. But the molar absorption coefficient of this low-energy band is very small compared to the MLCT absorption band of qdt and ecda complexes.

When excited at the charge-transfer absorption band, complexes **1**–**4** in degassed ethanol–methanol solution at 298 K exhibit weak luminescence consisting of a single broad and asymmetric band with a maximum between 870 and 925 nm. These complexes display excited state lifetimes ranging from 10 to 50 ns (Table 1). At room temperature, complexes **5**–**7** showed very weak and broad emission signals at >950 nm which did not allow for lifetime measurements under the same conditions. A very fast nonradiative decay rate is expected due to the low energy gap between the ground and excited states, which makes these complexes nonemissive at room temperature [25].

The absorption spectra of complexes **1**, **3** and **6** adsorbed on TiO_2 thin films are shown in Fig. 2. A comparison between Figs. 1 and 2 shows that the absorption spectra of the dyes in solution are similar to the spectra of the dyes adsorbed on the electrode, but the absorption bands of the dye on electrodes are broader and slightly red-shifted from the absorption spectra of the dyes in solution. This peak energy shift, as observed for many Ru-based complexes [6,12,17], may be due to the change in the energy levels of the ground and excited states compared to those in solution, due to the interaction between dye and the electrode.

The electrochemical data of the complexes measured in methanol solution are summarized in Table 1. All the complexes exhibit quasi-reversible oxidation wave for the

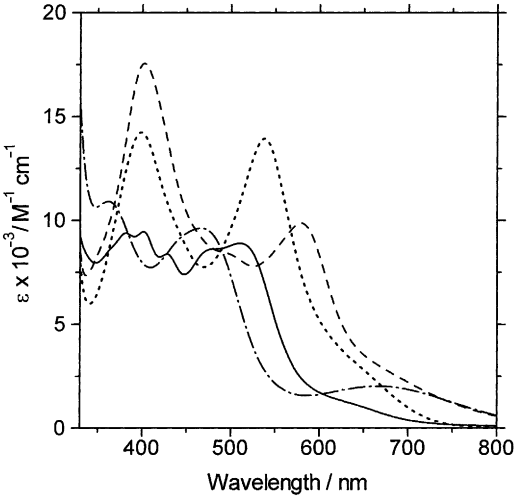

Fig. 1. Absorption spectra of Ru(dcbpy)$_2$(qdt) (—), Ru(dcbpy)$_2$(ecda) (– – –), Ru(dcbpy)$_2$(tdt) (—·—) and Ru(dcbpy)$_2$(NCS)$_2$ (- - -) in ethanol–methanol (4:1) solution at 298 K.

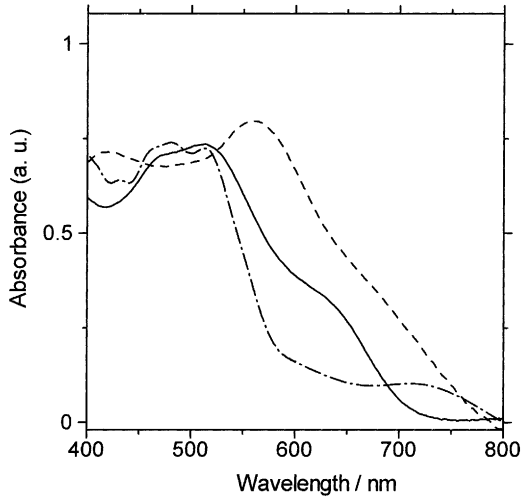

Fig. 2. Absorption spectra of Ru(dcbpy)$_2$(qdt) (—), Ru(dcbpy)$_2$(ecda) (– – –) and Ru(dcbpy)$_2$(tdt) (···) anchored to TiO_2 films. Spectra are corrected for absorbance of corresponding undyed films.

$Ru^{3+/2+}$ couple ranging from +0.27 to +0.86 V vs. SCE. The formation of an MLCT excited state of these complexes formally involves the oxidation of a HOMO having metal t_{2g} orbital character and reduction of a diimine-based LUMO. The ground state redox potentials listed in Table 1 show that the nature of the dithiolate influences the oxidation potentials. For the complexes studied, the energy of the acceptor orbital (LUMO) remains nearly constant and the decrease in MLCT transition energy arises mainly from the increase in the energy of the metal t_{2g} orbital (HOMO). The low-energy MLCT transitions in these complexes are consistent with $Ru^{3+/2+}$ oxidation potentials. The excited-state oxidation potential, $E^*_{1/2}(Ru^{3+/2+})$, indicates the measure of losing the electron that is placed in the π^* (diimine) LUMO upon excitation. For complexes **1–7**, $E^*_{1/2}(Ru^{3+/2+})$ values are estimated by Eq. (1) where$E_{1/2}(Ru^{3+/2+})$ is the oxidation potential of the ground state and E^{0-0} the energy difference between the lowest excited and ground states. The resulting $E^*_{1/2}(Ru^{3+/2+})$ values are shown in Table 1. The excited states of complexes **1–7** lie above the conduction band edge (−0.82 V vs. SCE) of the nanocrystalline TiO_2 [26]. Therefore, an efficient electron injection into the conduction band of the TiO_2 is expected for all these sensitizers **1–7**.

$$E^*_{1/2}(Ru^{3+/2+}) = E_{1/2}(Ru^{3+/2+}) - E^{0-0}\ (\text{in eV}) \quad (1)$$

3.2. Photoelectrochemical properties

Fig. 3 shows the photocurrent action spectra for complexes **1** and **3** adsorbed on TiO_2 electrodes where the incident photon to current conversion efficiency (IPCE) values are plotted as a function of wavelength. The IPCE at each incident wavelength were calculated from Eq. (2):

$$\text{IPCE}\ (\%) = \frac{1250 I_{ph}}{\lambda P_0} \times 100 \quad (2)$$

where I_{ph} is the photocurrent density at short circuit in $\mu A\,cm^{-2}$, λ the wavelength of incident radiation in nm, and

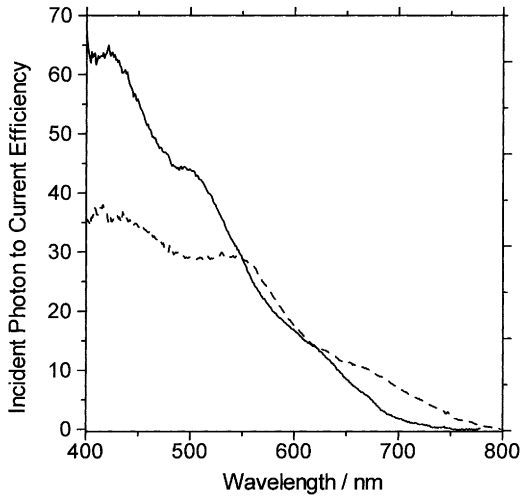

Fig. 3. Photocurrent action spectra of nanocrystalline TiO_2 films sensitized by complexes $Ru(dcbpy)_2(qdt)$ (—) and $Ru(dcbpy)_2(ecda)$ (– – –). The incident photon-to-current conversion efficiency is plotted as a function of wavelength. A sandwich type cell configuration was used to measure these spectra.

P_0 the photon flux in $W\,cm^{-2}$. A comparison between Figs. 2 and 3 shows that the photocurrent action spectra closely resemble the absorption spectra of the dyes adsorbed on TiO_2 electrode. The maximum IPCE values of complexes **1–5** at the lowest energy MLCT band are given in Table 2. The most efficient sensitizers in this series were the qdt complexes **1–2**, showing the IPCE value of 40–45% at 500 nm. However, their light harvesting at longer wavelengths (>650 nm) is very poor. In contrast, the red response was improved by replacing qdt with ecda or tdt while injection efficiencies were very low throughout the visible region (Fig. 3). The bdt and tdt complexes **5–7** showed a drastically reduced IPCE value of <7% at the lowest energy absorption band maxima.

Fig. 4 shows the photocurrent–voltage curves obtained under AM1.5 simulated illumination of the various dye-coated TiO_2 electrode systems studied in this work. The short-circuit photocurrent density (J_{sc}), open-circuit voltage (V_{oc}), fill factors (ff) and overall cell efficiencies

Table 2
Photoelectrochemical properties of $Ru(diimine)_2(dithiolate)$ sensitizers[a]

Sensitizer	$\Gamma \times 10^7$ (mol cm^{-2})[b]	LHE[c]	IPCE$_{max}$[c]	J_{sc} (mA cm^{-2})	V_{oc} (mV)	ff	η (%)
$Ru(dcbpy)_2(qdt)$	1.1	0.90	45	11.1	595	0.70	3.7
$Ru(dcphen)_2(qdt)$	1.6	0.98	40	10.0	595	0.67	3.2
$Ru(dcbpy)_2(ecda)$	2.2	0.99	30	5.4	580	0.65	2.0
$Ru(dcphen)_2(ecda)$	1.7	0.99	26	5.0	490	0.69	1.6
$Ru(dcbpy)_2(bdt)$	1.5	0.51	7	2.1	540	0.66	0.7
$Ru(dcbpy)_2(tdt)$	1.2	0.43	–	1.1	504	0.70	0.4
$Ru(dcphen)_2(tdt)$	1.3	0.56	–	0.4	470	0.60	0.2
$Ru(dcbpy)_2(NCS)_2$[d]	1.3	0.98	80	15.0	700	0.74	7.8

[a] TiO_2 thin films: 16 μm; light source: a solar simulator AM1.5 (100 mW cm^{-2}); electrolyte: 0.6 M DMPII + 0.05 M I_2 + 0.5 M TBP + 0.1 M LiI in acetonitrile; surface area of electrodes: 0.25 cm^2.

[b] Spectroscopically determined surface coverage of sensitizer.

[c] LHE and IPCE at the lowest energy absorption band maxima (Table 1).

[d] Data taken from Refs. [6,18].

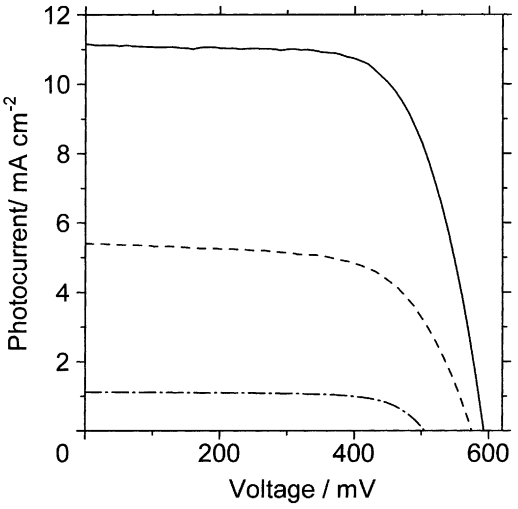

Fig. 4. Photocurrent–voltage characteristics of representative TiO_2 electrodes sensitized with dye: $Ru(dcbpy)_2(qdt)$ (—), $Ru(dcbpy)_2(ecda)$ (– – –) and $Ru(dcbpy)_2(tdt)$ (-·-·-).

(η) for each dye–TiO_2 electrode are reported in Table 2. The qdt complexes **1–2** show the best performance in this series. A short-circuit photocurrent of 11.1 mA cm^{-2} and an open-circuit potential of 595 mV with a fill factor of 0.70 were obtained for $Ru(dcbpy)_2(qdt)$, which corresponds to an overall efficiency of 3.7% (Table 2). Though ecda complexes **3–4** have superior panchromatic light harvesting properties to the $Ru(dcbpy)_2(NCS)_2$ sensitizer, they show poor overall photovoltaic performance. The bdt and tdt complexes **5–7** gave poorest results ($\eta < 0.7\%$).

The surface concentrations of the dye samples on TiO_2 films are estimated to be $1.1–2.2 \times 10^{-7}$ mol cm^{-2} (Table 2). The percent of light absorbed by the adsorbed chromophores is expressed as light-harvesting efficiency (LHE) which is related to the molar absorption coefficient by Eq. (3):

$$\mathrm{LHE}(\lambda) = 1 - 10^{-(1000\varepsilon\Gamma)} \quad (3)$$

where Γ is the surface coverage in mol cm^{-2} and ε the dye molar absorption coefficient in units of mol^{-1} cm^{-1} at wavelength λ. LHE of unity is ideal for a solar energy device as all the incident radiant power is collected. LHE at the low energy MLCT absorption maximum of the studied complexes are given in Table 2. For qdt and ecda complexes **1–4**, the LHE values are close to unity, but the IPCE values are only between 26 and 45%. The lower molar extinction coefficients for the bdt and tdt complexes **5–7** result in a lower LHE (≈0.5). The large differences in IPCE between the qdt and tdt sensitizers cannot be explained only by the changes in LHE.

IPCE is directly related to the LHE, the quantum yield of the charge injection (ϕ_{inj}), and the efficiency of collecting the injected charge at back contact (η_c), and is expressed by Eq. (4):

$$\mathrm{IPCE} = \mathrm{LHE}(\lambda)\phi_{inj}\eta_c \quad (4)$$

The excited state oxidation potential of all the sensitizers are sufficiently negative (<−0.93 vs. SCE) that it is expected to inject electrons efficiently into the conduction band of the nanocrystalline TiO_2 semiconductor. A very short lived MLCT excited state may compete with the electron injection rate. But the excited state lifetime of all dyes is in the nanosecond timescale which is about three orders of magnitude longer than the reported electron injection rate [27]. Therefore, ϕ_{inj} will be high and similar for all the sensitized-TiO_2 electrodes studied.

The recombination rates of injected electrons with the oxidized dye is an important factor affecting electron collection efficiency (η_c). The recombination rates will increase by changing the oxidation values to more negative potential. After electron injection, a competition is setup between charge recombination and iodide oxidation by oxidized dye. Considering the relative driving forces of these complexes, the charge recombination rates will increase in the order qdt < ecda < bdt ≈ tdt. The low injection efficiencies ($IPCE_{max}$ = 26–30%) of the ecda complexes compared to the qdt complexes can be explained by the fact that these complexes have $Ru^{3+/2+}$ ground state oxidation potential about 0.4 V more negative compared to those of the qdt complexes and the back reaction of injected electrons with Ru(III) comes to compete with the regeneration of Ru(II) through reaction with iodide. This effect will become more predominant in the bdt and tdt complexes where the $Ru^{3+/2+}$ potentials are very close to the I_3^-/I^- redox couple. Both bdt and tdt complexes show very low cell performance in this series, due to the high ratios of their rates of recombination to the rates of I^- oxidation. Because of this slow regeneration of Ru(II), backward electron transfer from TiO_2 to Ru(III) might become predominant in these processes. A low value of LHE is also responsible for the poor cell performance of these sensitizers.

Maximum injection efficiencies ($IPCE_{max}$) observed for the qdt complexes were only 40–45%, though redox potentials are obviously in a range to allow for efficient charge injection and dye regeneration, and hence are not responsible for reduced cell efficiencies. The main reason for the reduced $IPCE_{max}$ values of these complexes compared with the most efficient $Ru(dcbpy)_2(NCS)_2$ dye ($IPCE_{max}$ ≈ 80%) [6] is probably surface aggregation on the TiO_2 surface. Hence, further efforts would have to be taken in order to optimize in additives, electrolyte and redox mediator concentration for the qdt and ecda sensitizers.

4. Conclusions

Ruthenium(II) polypyridyl sensitizers with different dithiolate nonchromophoric ligands have been synthesized and characterized. The low energy metal-to-ligand charge-transfer transitions in these complexes have been tuned to about 150 nm by changing the donor strength of the dithiolate ligands to extend the spectral response

of nanocrystalline TiO_2 electrodes to longer wavelength values. Though qdt complexes have favorable ground and excited state energy levels to allow efficient charge injection and dye regeneration, the solar cell efficiencies of these new complexes were limited to 4%. This is due to reduced IPCE values (<45%) at 500 nm. Though ecda complexes **3–4** have superior panchromatic light-harvesting properties compared to the $Ru(dcbpy)_2(NCS)_2$ sensitizer, they show poor overall photovoltaic performance. A sluggish halide oxidation rate and a fast recombination of injected electron with the oxidized dye are likely responsible for the low cell efficiency of these complexes.

Acknowledgements

Financial support of this work by Science and Technology Agency, and Center of Excellence Development Project (COE), Japan is gratefully acknowledged.

References

[1] H. Tsubomura, M. Matsumura, Y. Nomura, T. Amamiya, Nature 261 (1976) 402.
[2] B. O'Regan, M. Grätzel, Nature 353 (1991) 737.
[3] C. Nasr, D. Liu, S. Hotchandani, P.V. Kamat, J. Phys. Chem. 100 (1996) 11054.
[4] J. Moser, M. Grätzel, J. Am. Chem. Soc. 106 (1984) 10769.
[5] K. Sayama, M. Sugino, H. Sugihara, Y. Abe, H. Arakawa, Chem. Lett. (1998) 753.
[6] Md.K. Nazeeruddin, A. Kay, I. Rodicio, R. Humphry-Baker, E. Müller, P. Liska, N. Vlachopoulos, M. Grätzel, J. Am. Chem. Soc. 115 (1993) 6382.
[7] R. Argazzi, C.A. Bignozzi, G.M. Hasselmann, G.J. Meyer, Inorg. Chem. 37 (1998) 4533.
[8] K. Sayama, H. Sugihara, H. Arakawa, Chem. Mater. 10 (1998) 3825.
[9] J. Desilvestro, M. Grätzel, L. Kavan, J. Augustynski, J. Am. Chem. Soc. 107 (1985) 2988.
[10] T.A. Heimer, C.A. Bignozzi, G.J. Meyer, J. Phys. Chem. 97 (1993) 11987.
[11] G. Sauvé, M.E. Cass, G. Coia, S.J. Doig, I. Lauermann, K.E. Pomykal, N.S. Lewis, J. Phys. Chem. B 104 (2000) 6821.
[12] A. Islam, H. Sugihara, K. Hara, L.P. Singh, R. Katoh, M. Yanagida, Y. Takahashi, S. Murata, H. Arakawa, New J. Chem. 24 (2000) 343.
[13] S. Ferrere, Chem. Mater. 12 (2000) 1083.
[14] G.M. Hasselmann, G.J. Meyer, Z. Phys. Chem. Bd. 212 (1999) 39.
[15] N. Alonso-Vante, J. Nieregarten, J. Sauvage, J. Chem. Soc., Dalton Trans. (1994) 1649.
[16] M. Grätzel, Current opinion in colloid, Interf. Sci. 4 (1999) 314.
[17] A. Islam, K. Hara, L.P. Singh, R. Katoh, M. Yanagida, S. Murata, Y. Takahashi, H. Sugihara, H. Arakawa, Chem. Lett. (2000) 490.
[18] M. Yanagida, L.P. Singh, K. Sayama, K. Hara, R. Katoh, A. Islam, H. Sugihara, H. Arakawa, Md.K. Nazeeruddin, M. Grätzel, J. Chem. Soc., Dalton Trans. (2000) 2817.
[19] Md.K. Nazeeruddin, P. Péchy, T. Renouard, S.M. Zakeeruddin, R. Humphry-Baker, P. Comte, P. Liska, L. Cevey, E. Costa, V. Shklover, L. Spiccia, G.B. Deacon, C.A. Bignozzi, M. Grätzel, J. Am. Chem. Soc. 123 (2001) 1613.
[20] A.C. Lees, B. Evrard, T.E. Keyes, J.G. Vos, C.J. Kleverlaan, M. Alebbi, C.A. Bignozzi, Eur. J. Inorg. Chem. (1999) 2309.
[21] Y. Takahashi, H. Arakawa, H. Sugihara, K. Hara, A. Islam, R. Katoh, Y. Tachibana, M. Yanagida, Inorg. Chim. Acta 12 (2000) 1083.
[22] K.A. Jensen, L. Henriksen, Acta Chem. Scand. 22 (1968) 1107.
[23] L.J. Theriot, K.K. Ganguli, S. Kavarnos, I. Bernal, J. Inorg. Nucl. Chem. 31 (1969) 3133.
[24] K. Hara, T. Horiguchi, T. Kinoshita, K. Sayama, H. Sugihara, H. Arakawa, Sol. Energ. Mater. Sol. C. 64 (2000) 115.
[25] R. Englman, J. Jortner, J. Mol. Phys. 18 (1970) 145.
[26] A. Hagfeld, M. Grätzel, Chem. Rev. 95 (1995) 49.
[27] Y. Tachibana, S.A. Haque, I.P. Mercer, J.R. Durrant, D.R. Klug, J. Phys. Chem. B 104 (2000) 1198.